Micro- and Nano-Patterned Copper Structures Using Directed Self-Assembly on Templates Fabricated from Phase-Separated Mixed Langmuir–Blodgett Films

ARTICLE *in* LANGMUIR · MAY 2008

Impact Factor: 4.46

9 AUTHORS, INCLUDING:

Satoshi Watanabe
Kumamoto University
26 PUBLICATIONS **195** CITATIONS
SEE PROFILE

Hirobumi Shibata
Chiba Institute of Technology
50 PUBLICATIONS **487** CITATIONS
SEE PROFILE

Masahiko Abe
Tokyo University of Science
630 PUBLICATIONS **7,125** CITATIONS
SEE PROFILE

Micro- and Nanopatterned Copper Structures Using Directed Self-Assembly on Templates Fabricated from Phase-Separated Mixed Langmuir−Blodgett Films

Satoshi Watanabe,[†] Hideto Kimura,[†] Takahiro Sato,[†] Hirobumi Shibata,[†] Fumitaka Sakamoto,[‡] Reiko Azumi,[§] Hideki Sakai,[||] Masahiko Abe,[||] and Mutsuyoshi Matsumoto*,[†]

Departments of Materials Science and Technology and of Pure and Applied Chemistry, Tokyo University of Science, Yamazaki 2641, Noda 278-8510, Thermo Fisher Scientific, Inc., 3-9 Moriya-cho, Kanagawa-ku, Yokohama 221-0022, and Photonics Research Institute, National Institute of Advanced Industrial Science and Technology (AIST), 1-1 Higashi, Tsukuba 305-8565, Japan

Received March 14, 2008. Revised Manuscript Received May 31, 2008

We report a versatile method to confine metal thin films in micro- and nanopatterns using directed self-assembly on the templates fabricated from phase-separated mixed Langmuir−Blodgett (LB) films. The pattern of the mixed LB films can be tuned by adjusting intermolecular interaction between the film-forming molecules in the LB films and by varying the fabrication conditions of the films such as the mixing ratio, subphase temperature, and surface pressure. We use the patterned LB films for templates to confine metal in patterned regions, taking advantage of the difference between the surface free energy of the patterned regions and that of the self-assembled monolayer of the silane coupling agent. Au nanoparticles are confined onto the patterned films as a catalyst for the succeeding Cu electroless deposition. The atomic force microscopic images, Auger electron spectra, and scanning Auger electron maps of a Cu-deposited film show that Cu is selectively deposited on the patterns of phase separation of the original mixed LB films.

Introduction

Surface patterning for the fabrication of structures defined at the micrometer and/or nanometer length scales has received increasing interest over the past few decades as a consequence of its potential applications in several scientific and technological fields, such as microelectromechanical systems (MEMSs),[1–3] photonic materials,[4,5] microchip reactors,[6] miniaturized sensors,[7,8] and separation techniques.[9–11] The ability to fabricate microscopic structures is important for creating functional nanoscale devices and novel materials. In this regard, a number of techniques have been invented and engaged in producing micrometer- or submicrometer-scale structures, such as conventional photolithography and electron beam lithography.[12,13] Photolithography and electron beam lithography have potential problems of increases in energy consumption and the size of the facilities. Microcontact printing is a typical process of soft lithography that defines a pattern by transferring a molecular ink from a patterned PDMS mold to a substrate, which can be termed chemical patterning.[14–16] Recent development of microscopic observation techniques, such as scanning probe microscopy for monolayers on solid substrates, enables us to directly observe micro- or nanoscale structures in films. A series of methods have also been developed to fabricate patterned, self-assembled monolayers, including dip-pen nanolithography,[17–19] scanning near-field photolithography,[20,21] and other scanning probe lithographies.[22,23]

Although efforts have been made to decrease the patterning size by the standard semiconductor lithography technology, fabricating nanostructured materials by "bottom-up" methods using self-assembling systems has been recognized as a powerful approach to establish novel nanolithography technologies. Block copolymers are well known to phase separate on a size scale

* To whom correspondence should be addressed. E-mail: m-matsu@rs.noda.tus.ac.jp.

[†] Department of Materials Science and Technology, Tokyo University of Science.

[‡] Thermo Fisher Scientific, Inc.

[§] AIST.

[||] Department of Pure and Applied Chemistry, Tokyo University of Science.

(1) Rogers, J. A.; Jackman, R. J.; Whitesides, G. W. *Adv. Mater.* **1997**, *9*, 475.
(2) Jackman, R. J.; Brittain, S. T.; Adams, A.; Prentiss, M. G.; Whitesides, G. W. *Science* **1998**, *280*, 2089.
(3) Liu, Y.; Klep, V.; Luzinov, I. *J. Am. Chem. Soc.* **2006**, *128*, 8106.
(4) Jiang, P.; Cizeron, J.; Bertone, J. F.; Colvin, V. L. *J. Am. Chem. Soc.* **1999**, *121*, 7957.
(5) Yan, X.; Yao, J.; Lu, G.; Chen, X.; Zhang, K.; Yang, B. *J. Am. Chem. Soc.* **2004**, *126*, 10510.
(6) Gau, H.; Herminhaus, S.; Lenz, P.; Lipowsky, R. *Science* **1999**, *283*, 46.
(7) Taton, T. A.; Lu, G. L.; Mirkin, C. A. *J. Am. Chem. Soc.* **2001**, *123*, 5164.
(8) Fendler, J. H. *Chem. Mater.* **2001**, *13*, 3196.
(9) Stein, A. *Microporous Mater.* **2001**, *44*, 227.
(10) Haidara, H.; Mougin, K.; Castelein, G.; Schultz, J. *Langmuir* **2000**, *16*, 9121.
(11) Gerding, J. D.; Willard, D. M.; Orden, A. V. *J. Am. Chem. Soc.* **2005**, *127*, 1106.
(12) Yin, D.; Horiuchi, S. *Langmuir* **2005**, *21*, 9352.
(13) Myers, B. D.; Dravid, C. P. *Nano Lett.* **2006**, *6*, 963.
(14) Gates, B. D.; Xu, Q.; Stewart, M.; Ryan, D.; Willson, C. G.; Whitesides, G. M. *Chem. Rev.* **2005**, *105*, 1171.
(15) Goh, C.; Coakley, K. M.; McGehee, M. D. *Nano Lett.* **2005**, *5*, 1545.
(16) Briseno, A. L.; Stefan, C.; Mannsfeld, B.; Ling, M. M.; Liu, S.; Tseng, R. J.; Reese, C.; Roberts, M. E.; Yang, Y.; Wudl, F.; Bao, Z. *Nature* **2006**, *444*, 14.
(17) Piner, R. D.; Zhu, J.; Xu, F.; Hong, S.; Mirkin, C. A. *Science* **1999**, *283*, 29.
(18) Weinberger, D. A.; Hong, S.; Mirkin, C. A.; Wessels, B. W.; Higgins, T. B. *Adv. Mater.* **2000**, *12*, 1600.
(19) Lee, S. W.; Oh, B.; Sanedrin, R. G.; Salaita, K.; Fujigaya, T.; Mirkin, C. A. *Adv. Mater.* **2006**, *18*, 1133.
(20) Sun, S.; Chong, K. S. L.; Leggett, G. J. *J. Am. Chem. Soc.* **2002**, *124*, 2414.
(21) Sundaramurthy, A.; Schuck, P. J.; Conley, N. R.; Fromm, D. P.; Kino, G. S.; Moerner, W. E. *Nano Lett.* **2006**, *6*, 355.
(22) Kramer, S.; Fuierer, R. R.; Gorman, C. B. *Chem. Rev.* **2003**, *103*, 4367.
(23) Coffey, D. C.; Ginger, D. S. *Nat. Mater.* **2006**, *5*, 735.

10.1021/la800805r CCC: $40.75
Published on Web 07/23/2008

determined by the block length, forming a variety of bicontinuous morphologies via molecular self-assembly, which can be controlled via synthesis and processing.[24,25]

The Langmuir−Blodgett (LB) technique has long been known to be a useful method for preparing organic monolayers on solid substrates. Compared with SPM-based lithography methods, the Langmuir−Blodgett-based preparation has the advantages of low cost, high throughput, and high density. Nanolath lattices consisting of stripes and channels with alternating wettability are fabricated by using wetting instabilities during the LB transfer.[26–28]

Laterally nanostructured materials have been fabricated using phase-separated structures in mixed LB films.[29–42] One of the methodologies for the fabrication of phase-separated structures in mixed LB films is to use two amphiphiles, one having an alkyl chain and the other having a perfluoroalkyl chain. The phase-separated mixed LB films have domains consisting of the former and the rest comprised of the latter. In the usual cases, domains are circular in shape and a few micrometers in diameter.[29–31,34–37,39–42]

We have communicated that domains at the nanometer length scale are formed in mixed LB films of fatty acid and hybrid carboxylic acid having both hydrogenated and perfluorinated portions in the hydrophobic part.[39] This is explained by assuming that the structures of the phase-separated LB films are governed by two competing interactions of line tension and dipole−dipole interaction. Line tension is a two-dimensional version of interface tension and favors the formation of large, circular domains. Dipole−dipole interaction in Langmuir and LB films is repulsive because molecules are aligned at a constant tilt angle. Circular domains at the micrometer length scale form when line tension is dominant. On the other hand, nanostructures form when dipole−dipole interaction is dominant. We have considered the effect of the chemical structures of the two components on the line tension, which should be approximately proportional to the difference between the homo- and heterointeractions. Line tension increases with an increase in the length of the alkyl chain of the fatty acid and with decreases in the lengths of the alkyl chain and perfluoroalkyl chain of the hybrid carboxylic acid. This provides us with a means to control the size of the domains in the mixed LB films. Using an amphiphilic silane coupling agent as one of the components of the mixed LB films, we can fabricate templates. The important point is that the phase-separated structures of the three-component mixed LB films reflect those of the two-component mixed LB films of fatty acid and hybrid carboxylic acid. When circular domains at the micrometer length scale form in mixed LB films of fatty acid and hybrid carboxylic acid, similar domain structures form in the three-component mixed LB films of the same fatty acid, the same hybrid carboxylic acid, and silane coupling agent. Nanostructures can be obtained in the three-component mixed LB films containing silane coupling agent by adjusting the fabrication conditions in the cases where nanostructures form in the two-component mixed LB films of the fatty acid and the hybrid carboxylic acid. Heat treatment of the three-component mixed LB films gives rise to the formation of a covalent bond between the silane coupling agent and a silanol group of the solid substrate. Rinsing the films with organic solvent yields selective removal of conventional amphiphiles such as fatty acid and hybrid carboxylic acid. The exdomain regions of the templates are the bare surfaces of the solid substrate with the rest covered with a self-assembled monolayer of perfluorinated silane coupling agent.[35–37,39–42]

In this study, we have fabricated three-component mixed LB films of fatty acid, hybrid carboxylic acid, and silane coupling agent. The phase-separated structures of the mixed LB films can be controlled by selecting the appropriate combination of the three components because the line tension of the domain walls should be approximately determined by the dispersive homo- and heterointeractions in the two-component mixed LB films of the fatty acid and the hybrid carboxylic acid. This allows us to design the size and shape of the patterns in the phase-separated LB films. Patterns are also affected by the fabrication conditions. Heat treatment of the mixed LB films followed by rinsing with organic solvent gives templates that reflect the patterns of the phase-separated mixed LB films. We have fabricated two types of phase-separated mixed LB films, one containing circular domains at the micrometer length scale and the other containing nanowires. We have fabricated two types of templates to confine the metal in designed regions, taking advantage of the difference between the surface free energy of the exdomain regions and that of the surrounding area (self-assembled monolayer of the silane coupling agent). We have employed electroless deposition (ELD) for the confinement of metal. This technique is a convenient and cheap method of depositing metal films on various solid substrates including nonconductive materials and does not require vacuum chambers or power supplies. ELD has been used for preparing thin metal films such as Au, Ag, Cu, Al, and Ni on solid substrates.[43–45] The structures of the metal-deposited films on the templates are investigated using atomic force microscopy (AFM) and Auger electron spectroscopy.

Experimental Section

Materials. The amphiphiles used in this study and the abbreviations are shown below. The numbers following F and H are the lengths of the perfluorocarbon and the hydrocarbon, respectively. "A" stands for a carboxylic group. Octadecanoic acid [$C_{17}H_{35}COOH$ (H17A)] and eicosanoic acid [$C_{19}H_{39}COOH$ (H19A)] were purchased from Fluka and Acros Organics, respectively. (Heptadecafluoro-

(24) Lopes, W. A.; Jaeger, H. M. *Nature* **2001**, *414*, 735.
(25) Kim, S. O.; Solak, H. H.; Stoykovich, M. P.; Ferrier, N. J.; Pablo, J. J.; Nealey, P. F. *Nature* **2003**, *424*, 24.
(26) Gleiche, M.; Chi, L. F.; Fuchs, H. *Nature* **2000**, *403*, 173.
(27) Lu, N.; Gleiche, M.; Zheng, J.; Lenhert, S.; Xu, B.; Chi, L. F.; Fuchs, H. *Adv. Mater.* **2002**, *14*, 1812.
(28) Zhang, M.; Lenhert, S.; Wang, M.; Chi, L. F.; Lu, N.; Fuchs, H.; Ming, N. *Adv. Mater.* **2004**, *16*, 409.
(29) Overney, R.; Meyer, M.; Frommer, E.; Brodbeck, J.; Luthi, D.; Howald, R.; Gunterodt, L.; Fujihira, H.-J.; Takano, M.; Gotoh, H. *Nature* **1992**, *359*, 133.
(30) Frommer, J.; Luthi, N/A.; Meyer, R.; Anselmetti, E.; Dreier, D.; Overney, M.; Gunterodt, R.; Fujihira, H.-J. M. *Nature* **1993**, *364*, 198.
(31) Overney, R.; Meyer, M.; Frommer, E.; Guntherodt, J.; Fujihira, H.-J.; Takao, M.; Gotoh, H. *Langmuir* **1994**, *10*, 1281.
(32) Duschl, C.; Liley, M.; Vogel, H. *Angew. Chem., Int. Ed. Engl.* **1994**, *33*, 1274.
(33) Ge, S.; Takahara, A.; Kajiyama, T. *Langmuir* **1995**, *11*, 1341.
(34) Iimura, K.; Shiraku, T.; Kato, T. *Langmuir* **2002**, *18*, 10183.
(35) Matsumoto, M.; Tanaka, M.; Azumi, R.; Manda, E.; Tachibana, H.; Kondo, Y.; Yoshino, N. *Mol. Cryst. Liq. Cryst.* **1997**, *294*, 31.
(36) Matsumoto, M.; Tanaka, K.; Kondo, Y.; Yoshino, N. *Chem. Lett.* **2002**, 970.
(37) Matsumoto, M.; Tanaka, K.; Azumi, R.; Kondo, Y.; Yoshino, N. *Langmuir* **2003**, *19*, 2802.
(38) Purrucker, O.; Fortig, A.; Ludtke, K.; Jordan, R.; Tanaka, M. *J. Am. Chem. Soc.* **2005**, *127*, 1258.
(39) Matsumoto, M.; Watanabe, S.; Tanaka, K.; Kimura, H.; Kasahara, M.; Shibata, H.; Azumi, R.; Sakai, H.; Abe, M.; Kondo, Y.; Yoshino, N. *Adv. Mater.* **2007**, *19*, 3668.
(40) Matsumoto, M.; Tanaka, K.; Azumi, R.; Kondo, Y.; Yoshino, N. *Langmuir* **2004**, *20*, 8728.
(41) Takahara, A.; Kojio, K.; Ge, S.; Kajiyama, T. *J. Vac. Sci. Technol., A* **1996**, *14*, 1747.
(42) Ge, S.; Takahara, A.; Kajiyama, T. *Langmuir* **1995**, *11*, 1341.
(43) Geissler, M.; Wolf, H.; Stutz, R.; Delamarche, E.; Grummt, U. W.; Michel, B.; Bietsch, A. *Langmuir* **2003**, *19*, 6301.
(44) Pesika, N. S.; Radisic, A.; Stebe, K. J.; Searson, P. C. *Nano Lett.* **2006**, *6*, 1023.
(45) Nadesalingam, M. P.; Mukherjee, S.; Somasundaram, S.; Chenthamarakshan, C. R.; Tacconi, N. R.; Rajeshwar, K.; Weiss, A. H. *Langmuir* **2007**, *23*, 1830.

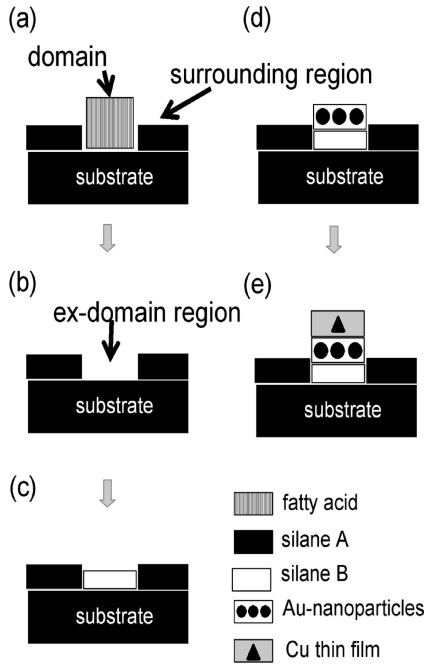

Figure 1. Preparation of the templates and electroless deposition of Cu on the templates: (a) transfer of phase-separated LB films, (b) preparation of templates by heat treatment and selective removal of conventional amphiphiles, (c) functionalization of the templates by forming self-assembled monolayers of silane coupling agent having an amino group, (d) immobilization of Au nanoparticles, (e) electroless deposition of Cu on the Au-nanoparticle-immobilized templates. The "domain", "surrounding region", and "exdomain region" are indicated.

1,1,2,2-tetrahydrodecyl)trimethoxysilane [$C_8F_{17}C_2H_4Si(OCH_3)_3$ (F8H2SiOMe)], (heptadecafluoro-1,1,2,2-tetrahydrodecyl)triethoxysilane [$C_8F_{17}C_2H_4Si(OC_2H_5)_3$ (F8H2SiOEt)], and (heptadecafluoro-1,1,2,2-tetrahydrodecyl)trichlorosilane [$C_8F_{17}C_2H_4SiCl_3$ (F8H2SiCl)] were obtained from Gelest Inc. 10,10,11,11,12,12,13,13,14,14,15,15,16,16,17,17,17-Heptadecafluoroheptadecanoic acid [$C_8F_{17}C_8H_{16}$-COOH (F8H8A)] was synthesized according to the literature.[46] 12,12,13,13,14,14,15,15,16,16,17,17,18,18,19,19,19-Heptadecafluorononadecanoic acid [$C_8F_{17}C_{10}H_{20}$COOH (F8H10A)] was purchased from Wako Pure Chemical Industries, Ltd. (3-Aminopropyl)trimethoxysilane (ApSiOMe) was obtained from Kanto Chemicals Co., Ltd. The compounds used in the preparation of Au nanoparticles and the Cu ELD bath are shown below. Chlorauric acid trihydrate, sodium citrate, sodium tetrahydroborate, copper(II) sulfate, Rochelle salt, and formaldehyde were purchased from Wako Pure Chemical Industries, Ltd.

Fabrication of LB Films. The monolayer measurements were performed using a Lauda Filmwaage (FW1) at 20 °C. The size of the trough available for the spreading was 15×50 cm^2. The spreading solvent was hexane for fatty acid and silane coupling agent and hexane/THF (99/1, v/v) for hybrid carboxylic acid. All the spreading solutions containing silane coupling agent were prepared under a nitrogen atmosphere. A spreading solution at a total concentration of 1.0×10^{-3} M was spread on pure water (electrical resistivity >18.2 MΩ). The molecules were compressed at a speed of 0.4×10^{-2} nm^2 molecule^{-1} min^{-1} after 30 min of evaporation time. Single-layer LB films were fabricated by transferring Langmuir films at 10 mN m^{-1} unless otherwise stated using the vertical dipping method at a withdrawal speed of 5 mm min^{-1} onto Si wafers with oxidized surfaces. The Si wafers were kept in aqueous NH_4OH and H_2O_2 at 98 °C for 10 min and rinsed with water before use.

ELD of Cu on the Templates. Figure 1 shows the scheme for the preparation of the templates and ELD of Cu on the templates. Samples were prepared as described below unless otherwise stated.

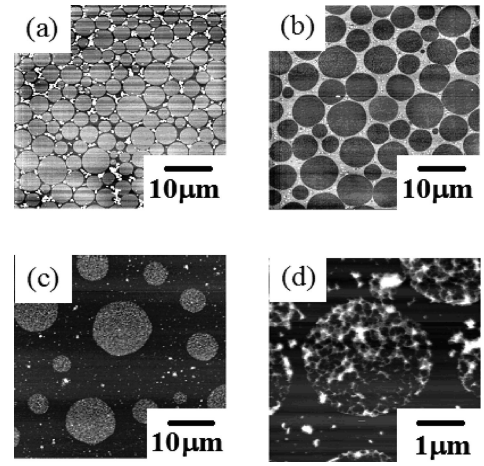

Figure 2. AFM images of (a) an as-deposited LB film of H19A and F8H2SiOEt at a molar ratio of 3/7, (b) the template fabricated by selective removal of H19A, (c) the Au-nanoparticle-immobilized template fabricated from a mixed LB film of H19A and F8H2SiCl at a molar ratio of 1/2 after selective removal of H19A, and (d) the electroless-deposited Cu film on the Au-nanoparticle-immobilized template (c).

Mixed LB films of conventional amphiphiles and silane coupling agent were fabricated (Figure 1a).

The mixed LB films were heated at 110 °C for 30 min, resulting in the formation of a covalent bond between the silane coupling agent and Si wafers. Then the mixed LB films were rinsed with ethanol for selective removal of the conventional amphiphiles (Figure 1b). The templates were functionalized by immersion in 10 mM ApSiOMe in methanol for 12−24 h to form self-assembled monolayers of ApSiOMe (Figure 1c). Au nanoparticles with a diameter of 4 nm were prepared by using the recipe of Y. Jin.[47] A 50 mL volume of pure water was mixed with 1 mL of 1 wt % aqueous $HAuCl_4 \cdot 3H_2O$, and 1 mL of 1 wt % aqueous sodium citrate was added. While the mixture was vigorously stirred, 1 mL of 0.075 wt % aqueous $NaBH_4$ was added. After the appearance of a deep red color, stirring was continued for 5 min. Au nanoparticles were immobilized on the functionalized templates by immersing the templates in an aqueous solution of Au nanoparticles for 1 h at room temperature (Figure 1d). Cu solutions were prepared by dissolving 0.2 g of $CuSO_4$, 0.2 g of Rochelle salt, and 0.3 g of NaOH in 50 mL of pure water at 40 °C. A 10 mL portion of 36−38 wt % formaldehyde was added to 50 mL of the Cu solution to supply the reducing agent to the plating bath. Cu electroless plating baths were prepared immediately prior to plating the samples. Patterned samples of Au nanoparticles were immersed in the Cu plating bath for 1−30 min at 40 °C. Plating was stopped by removing the sample from the bath and rinsing it with pure water (Figure 1e).

Instrumentation. Topographic measurements were performed with an SPA 300 microscope (SII, Japan). Noncontact mode topographic images were acquired at a scan rate of 1 Hz using silicon nitride cantilevers with a spring constant of 15 N m^{-1} and a resonance frequency of 127 kHz. Scanning Auger micrographs were acquired on a Microlab350 (Thermo Fisher Scientific) with a field emission electron source. Most SEM images, Auger electron spectra, and Auger elemental maps were taken using a 10 kV electron beam. For Si and C, the KLL transitions are at 1620 and 275 eV, respectively. To obtain scanning Auger Cu maps, the MNN transition at 920 eV was used.

Results and Discussion

Cu Deposition on Templates with Patterns at the Micrometer Length Scale. First, we studied Cu deposition on templates with microscopic patterns. Figure 2a shows the AFM

(46) Requirand, N.; Blancou, H.; Commeyras, A. *Bull. Soc. Chim. Fr.* **1993**, *130*, 798.

(47) Jin, Y.; Kang, X.; Song, Y.; Zhang, B.; Cheng, G.; Dong, S. *Anal. Chem.* **2001**, *73*, 2643.

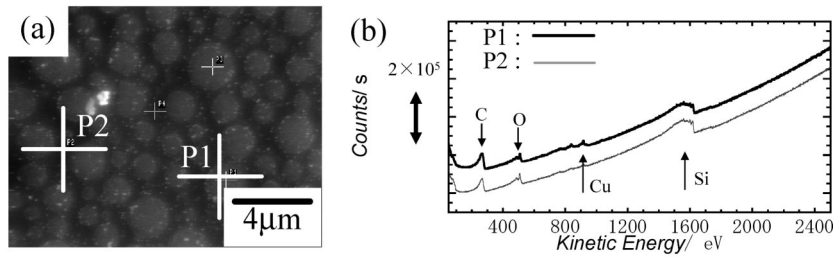

Figure 3. (a) SEM image and (b) Auger electron spectra of a Cu-electroless-deposited film. The crosses in (a) show the positions for the Auger electron spectra given in (b).

image of an as-deposited mixed LB film of H19A and F8H2SiOEt at a molar ratio of 3/7. Circular domains at the micrometer length scale are evident in the LB film. The domain shape and size are dominated by the line tension. The domains should consist of H19A, and the surrounding region should be comprised of F8H2SiOEt. The height of the domains is larger than the surrounding region by ca. 1.5 nm. This value is almost coincident with the difference between the molecular length of H19A and that of F8H2SiOEt in stretched forms. The area fraction of the domains increases with an increase in the molar fraction of H19A, indicating that the brighter domains and the surrounding region should be attributed to the region of H19A and the region of F8H2SiOEt, respectively.

Figure 2b shows an AFM image of the template fabricated by heating the mixed LB film, followed by rinsing the film with ethanol. It is clear that the material in the domain region has been selectively removed. The exdomain region is lower than the surrounding region by ca. 1 nm. This shows that H19A was selectively removed by the heating and rinsing processes. The exdomain region of the template should be the bare surface of the oxidized Si wafer and be hydrophilic, while the surrounding region should be covered with a hydrophobic self-assembled monolayer of F8H2SiOEt. This enables us to functionalize selectively the exdomain region, with the surrounding region remaining intact.

The SAM of ApSiOMe was formed on the exdomain region of the template by liquid-phase adsorption to fabricate a functionalized template. The exdomain region was lower than the surrounding region by about 0.5 nm (data not shown) due to the formation of the SAM, with amino groups protruding from the surface of the exdomain region.

Figure 2c shows the AFM image of a Au-nanoparticle-immobilized film fabricated by immersing in a solution of Au nanoparticles a functionalized template obtained from a mixed LB film of H19A and F8H2SiCl at a molar ratio of 1/2. The immersion of the functionalized template in the Au nanoparticle solution gives rise to a selective immobilization of Au nanoparticles on the exdomain region due to the electrostatic interaction between the amino groups of the functionalized part of the template and citrate anions surrounding the Au nanoparticles. After the immobilization the exdomain region is higher than the surrounding region by ca. 1 nm. This shows that Au nanoparticles were confined on the functionalized part of the template. The immobilization of Au nanoparticles gave rise to an increase in height of the functionalized part of the template by ca. 2 nm, which is consistent with the diameter of the Au nanoparticles.

Figure 2d shows the AFM image of an electroless-deposited Cu film with an immersion time of 5 min on the Au-nanoparticle-immobilized template shown in Figure 2c. The height of the domain region increases by ca. 30 nm during the ELD. It is evident that Cu grows selectively on the Au-nanoparticle-immobilized part. This is because the immobilized Au nanoparticles act as catalysts for the ELD of Cu with formaldehyde as a reducing agent.

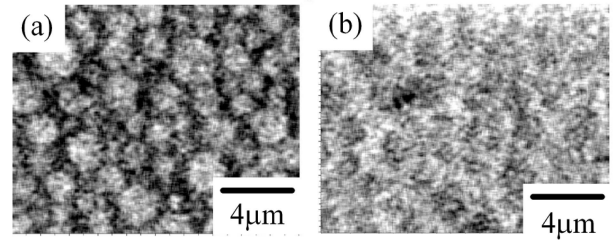

Figure 4. Scanning Auger electron maps of (a) Cu and (b) Si of a Cu-electroless-deposited film.

To corroborate the selective deposition of Cu on the exdomain region, we have performed elemental analyses of Cu-deposited films using Auger electron spectroscopy and scanning Auger elemental mapping. An SEM image and Auger electron spectra of a Cu-deposited film are shown in Figure 3.

The SEM image shown in Figure 3a is consistent with the AFM results in that circular domains at a micrometer length scale are present in the film. The secondary electrons are emitted more efficiently from the exdomain region than the surrounding region. This agrees with the AFM results that Cu is selectively deposited on the exdomain region. Positions P1 and P2 shown as crosses in Figure 3a correspond to the exdomain region and the surrounding region, respectively. Figure 3b shows the Auger electron spectra of the materials at P1 and P2. The signals in the spectrum of the material at P1 are assigned as follows: C (KLL, 269 eV), O (KLL, 502 eV), Cu (LMM, 920 eV), Si (KLL, 1600 eV).[48,49] The spectrum of the material at P2 is similar to that at P1 except for the absence of a signal due to Cu. This shows that Cu is selectively deposited on the exdomain region of the film. The signal assigned to carbon in the spectrum of the material at P1 should be due to carbon atoms derived from ApSiOMe and sodium citrate on the surface of Au nanoparticles, while that in the spectrum of the material at P2 should be due to carbon atoms derived from F8H2SiOEt.

Scanning Auger electron maps of Cu and Si are shown in parts a and b, respectively, of Figure 4. Figure 4a clearly shows that Cu exists predominantly in the exdomain region. This supports the AFM results that Cu grows selectively on the exdomain region during the ELD. Figure 4b shows that Auger electrons are less efficiently emitted from the exdomain region than from the surrounding region. This should be due to the presence of Cu on the exdomain region.

(48) Sheng, H. Y.; Fujita, D.; Dong, Z. C.; Okamoto, H.; Ohgi, T.; Nejoh, H. *J. Vac. Sci. Technol., B* **1999**, *17*, 2565.
(49) Galtayries, A.; Bonnelle, J.-P. *Surf. Interface Anal.* **1995**, *23*, 171.

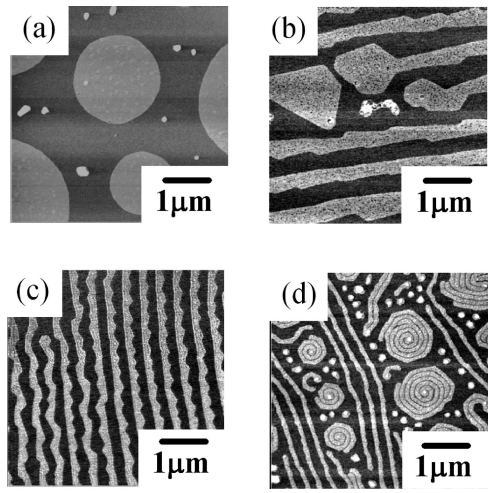

Figure 5. AFM images of mixed LB films of H19A/F8H10A/F8H2SiOMe at molar ratios of 9/*x*/27 transferred at 10 mN m^{-1} at 20 °C: (a) $x = 0$, (b) $x = 1$, (c) $x = 1.5$, (d) $x = 3$.

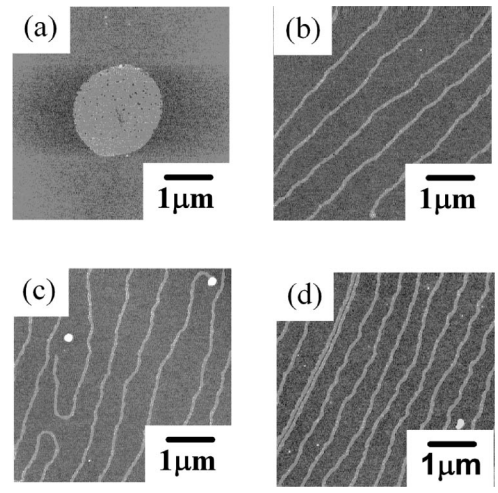

Figure 6. AFM images of mixed LB films of H17A/F8H8A/F8H2SiOEt at a molar ratio of 2/2/5 transferred at 10 °C. The transfer pressure is (a) 2, (b) 4, (c) 6, and (d) 8 mN m^{-1}.

Cu Deposition on Templates with Patterns at the Nanometer Length Scale. We have reported that the domains with the shape of nanowires are formed in mixed LB films of fatty acid and hybrid carboxylic acid having both hydrogenated and perfluorinated alkyl parts.[39] By adjusting the hydrophobic parts of the fatty acid and hybrid carboxylic acid and by adjusting the fabrication conditions, we can control the size of the domains. Adding silane coupling agent as a third film-forming material yields phase-separated mixed LB films that can be converted to templates as shown above. The combination of fatty acid, hybrid carboxylic acid, and silane coupling agent as well as the variation in the fabrication conditions leads to a variety of phase-separated structures such as circular domains at the micrometer length scale, nanowires, and spirals.

First, we have examined the effect of the molar fraction of hybrid carboxylic acid on the phase-separated structures of mixed LB films. Figure 5 shows the AFM images of the mixed LB films of H19A/F8H10A/F8H2SiOMe at molar ratios of 9/*x*/27 transferred at 10 mN m^{-1} at 20 °C. We have employed the combination of H19A and F8H10A because well-defined nanowires form in the mixed LB films of H19A and F8H10A. Figure 5a shows that circular domains at the micrometer length scale form in the absence of F8H10A. The addition of F8H10A gives rise to the formation of wire-type domains (Figure 5b). Nanowires form in the phase-separated LB films with $x = 1.5$ as shown in Figure 5c. When the molar fraction of F8H10A is large ($x = 3$), spirals form as in the mixed LB films of H17A/F8H10A/F8H2SiOEt at a molar ratio of 9/1/10.[39] These results demonstrate that the addition of hybrid carboxylic acid allows for the formation of nanostructures in the case where nanostructures form in the two-component mixed LB films of the fatty acid and the carboxylic acid.

Next, we have investigated the phase-separated structures of mixed LB films containing F8H2SiOEt. Figure 6 shows the AFM images of mixed LB films of H17A/F8H8A/F8H2SiOEt at a molar ratio of 2/2/5 transferred at varying surface pressures at 20 °C. We have employed the combination of H17A and F8H8A because this combination gives well-defined nanowires in the two-component mixed LB films. Figure 6a shows that circular domains at the micrometer length scale form at a surface pressure of 2 mN m^{-1}. The circular domains are converted into nanowires at higher surface pressures as shown in Figure 6b−d. This is understood by considering the change in orientation of H17A at the air−water interface during compression. With compression molecules of H17A will be oriented in a more organized manner with a smaller distribution in the tilt angle. This gives rise to an increase in the contribution of dipole−dipole interaction to the phase-separated structures of mixed LB films, favoring the formation of nanostructures at high surface pressures. Transition from circular domains to nanowires with compression was also observed in mixed LB films of H17A/F8H8A/F8H2SiOEt at different molar ratios and in those of H19A/F8H10A/F8H2SiOMe at a molar ratio of 9/1.5/27.

We have fabricated mixed LB films of H19A/F8H10A/F8H2SiOEt at a molar ratio of 9/1/20 at a surface pressure of 5 mN m^{-1} at 20 °C. We have employed this system to fabricate templates for patterning because well-defined nanowires form in mixed LB films of H19A and F8H10A. Further we have employed a small molar fraction of F8H10A because of the possibility of F8H10A in the region of F8H2SiOEt, which may blur the domain boundaries. The AFM image of an as-deposited film is shown in Figure 7a.

The formation of nanowires in the mixed LB film is evident. The average width of the nanowires is 101 nm with a standard deviation of 7 nm. The cross-sectional view of the AFM image is shown in Figure 7b. The height of the domains is higher than that of the surrounding region by ca. 1.5 nm, which is similar to the results of mixed LB films of H19A/F8H2SiOEt at a molar ratio of 3/7. The domains should consist of H19A surrounded by F8H10A and F8H2SiOEt. F8H10A should be positioned at the domain boundaries.

The mixed LB films were subjected to heat treatment and rinsing to form templates. The templates were functionalized with ApSiOMe, followed by immobilization of Au nanoparticles at a concentration half that described in the Experimental Section. ELD of Cu was performed using a Cu plating bath at 40 °C with an immersion time of 30 min. The concentration of the Cu plating bath was a 1/10 that described in the Experimental Section. The AFM image and the cross section of the Cu-deposited film are shown in parts c and d, respectively, of Figure 7. It is evident that nanowires are present even after the ELD. The ELD gives rise to an increase in height of the exdomain region by ca. 5 nm. The average width of the Cu nanowires was 105 nm with a standard deviation of 8 nm. The average width and the standard deviation are not very different from those of the nanowires in the as-deposited mixed LB films. When phase-separated mixed LB films of H19A/F8H10A/F8H2SiOMe at a molar ratio of

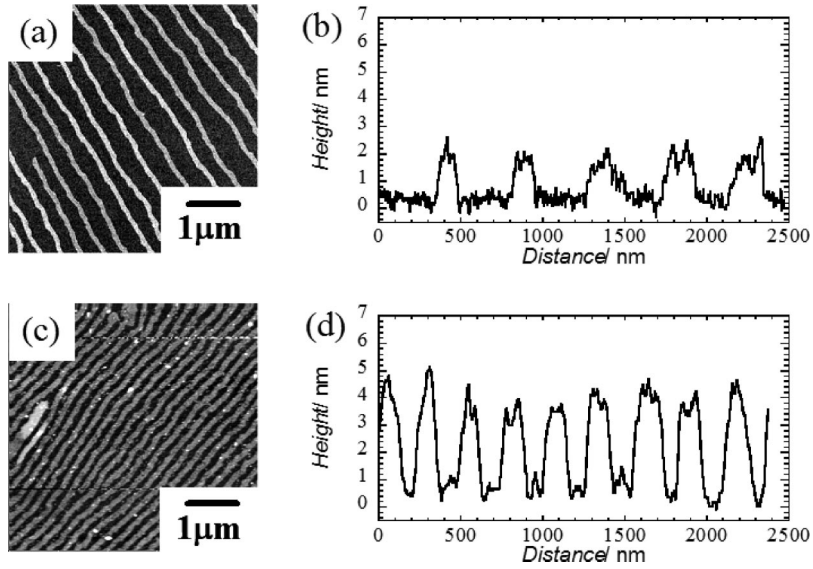

Figure 7. (a) AFM image of an as-deposited LB film of H19A/F8H10A/F8H2SiOEt at a molar ratio of 9/1/20 transferred at a surface pressure of 5 mN m^{-1} at 20 °C and (b) cross-sectional view of (a). (c) AFM image of the Cu-deposited film and (d) cross-sectional view of (c).

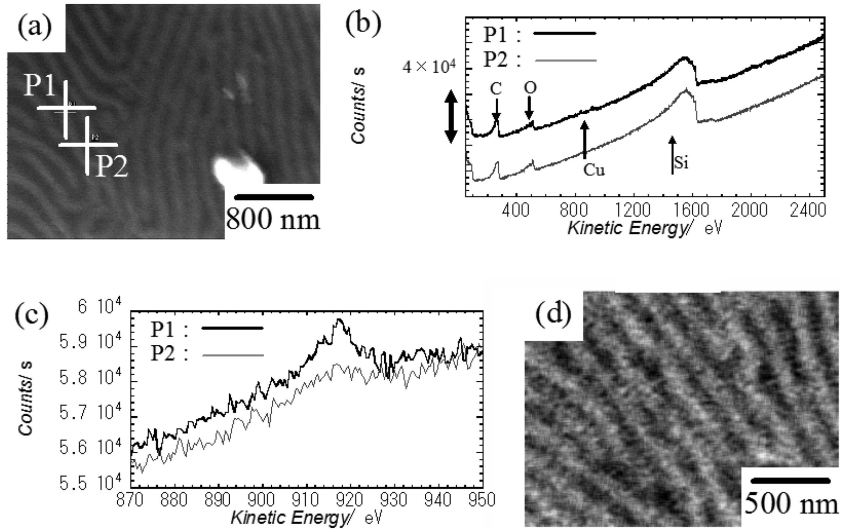

Figure 8. (a) SEM image and (b) Auger electron spectra of a Cu-deposited film fabricated from a mixed LB film of H19A/F8H10A/F8H2SiOEt at a molar ratio of 9/1/20 transferred at a surface pressure of 5 mN m^{-1} at 20 °C. The crosses in (a) show the positions for the Auger electron spectra given in (b). (c) Auger electron spectra of Cu and (d) a scanning Auger electron map of Cu of the Cu-deposited film.

3/1/20 were fabricated, the average width of the nanowires was 120 nm with a standard deviation of 10 nm. Functionalized templates were fabricated using the above mixed LB films. In this case, ELD of Cu was carried out using a Cu plating bath at a concentration the same as that described in the Experimental Section to increase the thickness of the Cu nanowires. Using an immersion time of 2 min, the thickness of the Cu nanowires was ca. 20 nm and the average width was 150 nm with a standard deviation of 13 nm. When the immersion time was 4 min, the thickness of the Cu nanowires was ca. 80 nm and the average width was 188 nm with a standard deviation of 16 nm. The average width of the Cu nanowires increases with increasing thickness, showing that Cu deposition occurs not only in the vertical direction but also in the horizontal direction. The thickness of the Cu nanowires was not proportional to the immersion time, suggesting the difficulty of thickness control by the immersion time under the experimental conditions. These results indicate that nanowires of Cu can be obtained using templates fabricated from phase-separated mixed LB films.

An SEM image of a Cu-deposited film fabricated from a mixed LB film of H19A/F8H10A/F8H2SiOEt at a molar ratio of 9/1/20 transferred at a surface pressure of 5 mN m^{-1} at 20 °C is shown in Figure 8a. This image also shows the presence of nanowires.

Positions P1 and P2 shown as crosses in Figure 8a correspond to the exdomain region and the surrounding region, respectively. Figure 8b shows Auger electron spectra of the materials at P1 and P2. The spectrum of the material at P2 is similar to that at P1 except for the signal due to Cu. Figure 8c shows the Auger electron spectra of Cu. It is evident that the signal of Cu is much stronger in the spectrum of the material at P1 than that at P2, showing that Cu is predominantly deposited on the exdomain region of the film. Auger electron spectra of Cu (LMM) should have three peaks at 776, 840, and 920 eV.[49] In the spectrum of the material at P1, only a single peak at 917 eV appears. This peak should be due to copper oxides[49] such as Cu_2O and CuO formed by the oxidation of Cu. The oxidation of Cu should be effective in the surface region. Due to the thickness of the nanowires of Cu as small as 5 nm, most of the copper in the

nanowires exists as oxides. A scanning Auger electron map of Cu at 917 eV of the Cu-deposited film is shown in Figure 8d. This figure clearly shows that Cu exists predominantly in the exdomain region. This is strong evidence of the selective growth of Cu on the exdomain region during the ELD. The width of the nanowires in the scanning Auger electron map is larger than that in the AFM image because the size of the electron beam is several tens of nanometers. These results clearly indicate that nanowires of Cu can be obtained using templates fabricated from phase-separated mixed LB films.

Conclusions

We have demonstrated a versatile method for the formation of Cu patterns on the templates fabricated from phase-separated mixed LB films. The pattern of the templates can be tuned by adjusting the intermolecular interaction between the film-forming molecules and by adjusting the fabrication conditions of the films. Patterns such as circles at the micrometer length scale and nanowires are easily formed. Fabrication of Cu patterns consists solely of self-assembling processes such as phase separation, liquid-phase adsorption to form SAMs, immobilization of Au nanoparticles using electrostatic interaction, and ELD of Cu. The present method provides a fast and easy route for obtaining chemically patterned surfaces with different surface chemical activities and has potential application in parallel nanofabrication, with a low cost and high throughput. Further study is now in progress to widen the prospect of the present method.

Acknowledgment. This work was partly supported by the Japan Society for the Promotion of Science (Grant No.18350077).

LA800805R